Astron. Astrophys. 55, 299—302 (1977)

ASTRONOMY AND ASTROPHYSICS

Strip Photometry of Diffuse Objects

I. The Structure of Comets Kohoutek (1973 XII) and Bradfield (1974 III)

Federico M. Strauss

Instituto de Fisica, Universidade Federal do Rio Grande do Sul, 90.000 Porto Alegre-RS, Brasil

Received July 23, revised September 9, 1976

Summary. A high signal to noise ratio and good one dimensional resolution are obtained by scanning a narrow slit across extended objects. Several observations of two comets give information on total brightness and on the density distribution of the coma. The characteristic scale length reduced to 1 AU of the coma of comet Bradfield was $10^{4.8\pm0.1}$ km, in agreement with that of C_2 in comet Bennet (1970 II) obtained by Delsemme and Moreau (1973). For comet Kohoutek we obtained a slightly larger value, $10^{5.0\pm0.1}$ km.

Key words: photometry — comets

I. Introduction

The photometry of diffuse objects requires a compromise between resolution and signal to noise (S/N) ratio. Strip photometry is a technique in which a long and narrow slit is scanned across an image. This technique may provide both good resolution in one dimension together with good S/N, by using a narrow slit of large total area. Substraction of sky and instrumental background is accomplished by fitting a baseline to both ends of the scan, and spikes due to isolated stars may be deleted. This method was used e.g. by Houten et al. (1954) who scanned several galaxies. Area scanners (e.g. Rakos, 1965) which make repetitive fast scans are intended primarily for high resolution photometry of small objects (of a few seconds of arc) blurred by atmospheric seeing. For long bright objects (such as the two comets we have observed) a single scan contains much information both on structural details and on integrated properties.

II. Instrument

The observations were made on a 50 cm aperture, $f:13.3$ Cassegrain telescope. The photometer, using an EMI 9658 photomultiplier tube and pulse-counting equipment, had its digital output on a fast line-printer. The knife-edge slit had a width of 6″.3 and an effective length between half-sensitivity points of 8′. Two scanning speeds were available, namely $15''.04\cos\delta\ s^{-1}$ and $1''.22\cos\delta\ s^{-1}$, using respectively 0.1 and 1 s counting times per sample, with a gap of 41.5 ms between samples.

III. Calibration and Analysis of Scans

Scanning an extended object along the x-axis with a long slit oriented parallel to the y-axis we obtain $I(x)$ which is the convolution of the brightness distribution with the rectangular beam. If the length of the slit exceeds the size of the object, the integral of $I(x)$ is proportional to the total brightness. When an extended object and a comparison star at the same declination and zenith distance are scanned under the same atmospheric and instrumental conditions, the ratio of their integrated scans equals the ratio of their intensities.

Figure 1 shows a portion of a scan of comet Bradfield (1974 III) obtained on 18 March 1974, a few hours after perihelion. Also shown is a scan of a nearby comparison star made about two minutes earlier at the same air mass. The count rates were corrected for dead time and the sky background was substracted; a numerical filter described below was applied to the data. Poor seeing due to the large zenith distance has widened the instrumental response as shown by the star's scan, which may be approximated by a gaussian. Therefore, we have applied Bracewell's (1955) chord construction to restore the comet's scan to nearly its true shape. Outside the central peak, the effect of restoration is negligible, as shown in Figure 1.

As a first approximation the sunward hemisphere of the coma may be described as having spherical symmetry, at least down to the brightness limit of our observations. The amount of light emitted per unit volume is proportional to σn, the product of the cross section and the number density of the emitting particles in the coma. If the optical depth is small, the restored intensity is the integral along a slice of the coma,

$$I(x)=A\int\int \sigma n\,dy\,dz \qquad (1)$$

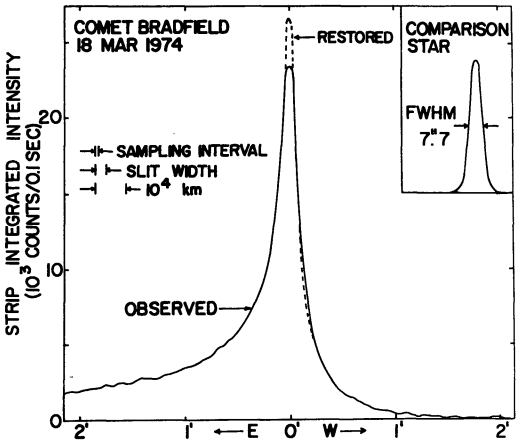

Fig. 1. Portion of a $W \rightarrow E$ scan of comet Bradfield (1974 III) at perihelion, consisting of 120 samples obtained in 17 s. The full scan lasted 145 s; a linear baseline fitted to both ends of the scan, amounting to 19% of the peak intensity, was removed from the data. The restored curve is the result of correcting for the finite resolution of the system. Inset: portion of a scan of the seventh magnitude comparison star HD 11351, drawn to the same scale

Table 1. Results. Integrated brightness m (observed) and M (reduced to an Earth-comet distance $\Delta = 1$ AU), as a function of heliocentric distance r. The characteristic scale length s_0, determined by fitting model b, is given in angular and linear units; its uncertainty is estimated at $\pm 20\%$

Comet	Date	r	Brightness		s_0	
	1974 (UT)	(AU)	m	M	(′)	(10^3 km)
Kohoutek	Jan. 11.992	0.546			0.8	30
(1973 XII)	13.983	0.602	4.9	5.3	1.2	43
	16.988	0.680	4.6	5.0	1.6	57
	19.985	0.758	5.8	6.3	1.7	61
	30.987	1.019	7.2	7.3	2.0	85
Bradfield	Mar. 12.948	0.521	5.2	5.4	0.4	16
(1974 III)	13.952	0.514	4.8	5.1	0.5	19
	18.948	0.503	4.1	4.6	0.4	14
	21.945	0.511	3.9	4.5	0.6	19

where the z-axis runs along the line of sight and A is a proportionality constant. If σn depends only on the distance R of a volume element to the nucleus, this integral equation may be inverted using Plummer's formula (Sawyer-Hogg, 1959, p. 175), obtaining

$$\sigma n = \frac{-1}{2\pi A x} \frac{dI(x)}{dx} \tag{2}$$

where x, measured from the nucleus, is to be set equal to R. The derivative may be replaced by finite differences and the constants set aside as follows:

$$\log(\sigma n)_{\bar{x}=R} \simeq \log\left[\frac{I(x_i) - I(x_{i+1})}{(x_{i+1} - x_i)\bar{x}}\right] + \text{constant} \tag{3}$$

with $\bar{x} = 0.5\,(x_i + x_{i+1})$. The origin $x = 0$ is taken at the position of peak brightness of the scan, which may be determined by graphical interpolation with an accuracy of a fraction of the sampling interval a.

Since Equation (2) depends only on dI/dx and not on $I(x)$, an error in estimating the background level does not affect the result.

Both Equation (3) and the restoration process are high-pass filters which enhance the noise near the Nyquist frequency. Therefore, we have applied a numerical low-pass filter consisting of a five point running average of the data with weights ($-1/16$, 1/4, 5/8, 1/4, $-1/16$). The transfer function of this filter in terms of the spacial frequency ω is

$$F(\omega) = 1 - \sin^4(\pi a \omega). \tag{4}$$

At the Nyquist frequency $\omega_N = (2a)^{-1}$ we have $F(\omega_N) = 0$, while the low frequencies are practically unaffected. Further, the standard deviation of the noise in $I(x)$ is reduced by a factor 0.72; this is equivalent to doubling the integration time, with less loss in resolution.

IV. Results and Discussion

We have made several observations of comets Kohoutek (1973 XII) and Bradfield (1974 III). To obtain a stronger signal, no filter was used and therefore the magnitudes will be affected by an unknown color correction. The large air mass shifts the instrumental effective wavelength towards the red, giving nearly visual response; our integrated magnitudes are directly comparable with eye estimates. Table 1 gives the total apparent magnitude m and the total reduced magnitude M of the comets, where the latter refers to a standard Earth-comet distance $\Delta = 1$ AU. Our results for comet Kohoutek average slightly fainter than the total visual brightness data compiled by Jacchia (1974) and Angione et al. (1975), probably because our scans missed part of the tail (see below). We confirm the standstill in the decline around January 17 found by Angione et al. (1975).

Equation (3) was applied to the scan of comet Bradfield shown in Figure 1, sunwards of the nucleus. The run of $\log(\sigma n)$ is plotted in Figure 2, as a function of the radius R expressed both in arc min and in km. At small R we show both the restored and the unrestored data; for larger R the noise level increases and we have averaged first five and later ten consecutive data points before applying Equation (3). In all we follow the coma out to about $6\,10^4$ km through a range of σn of some five orders of magnitude. Similarly Figure 3 shows $\log(\sigma n)$ from a scan of comet Kohoutek. The coma is much less concentrated, extending four times farther for the same drop in intensity than the coma of comet Bradfield, and restoration was unnecessary. According to Baum (1962), one way to reduce the deterioration of S/N toward the outskirts is to increase the sampled area. We averaged a progressively increasing number of consecutive data points, starting with a single point at the peak, followed

by the average of the next two, followed by that of the next three, etc., before applying Equation (3).

We have attempted to fit the data of Figures 2 and 3 by three well known coma models. Assuming that the particles leave the nucleus isotropically, moving radially at constant velocity v, the product σn will depend on the distance R to the nucleus. The three models are:

a) A flow of non-decaying dust particles, with σ = constant and $n \propto R^{-2}$.

b) A flow of molecules that are dissociated by the solar UV or particle flux with a lifetime τ, corresponding to a scale length $s_0 = v\tau$, with σ = constant and

$$n \propto R^{-2} \exp(-R/s_0).$$

c) An icy-grain halo of vaporizing grains, extending out to a distance R_H, with $\sigma \propto (1 - R/R_H)^2$ and $n \propto R^{-2}$ (Delsemme and Miller, 1971).

Figures 2 and 3 show that model *a* fits the data only for values of σn greater than about 10^{-2} of that found in the central regions; model *b* is adequate throughout, while model *c* may be good down to 10^{-4}. Thus, model *a* may be rejected as the source of the radiation detected by us, while it is more uncertain to choose between *b* and *c*. This is the same conclusion reached by Delsemme and Moreau (1973) in the case of comet Bennet (1970 II). Although the icy-grain model gives a passable fit to the data, it is unlikely because the required extent of the halo ($R_H = 43\,10^3$ km for Figure 2 and $140\,10^3$ km for Figure 3) is much larger than that predicted by the theory of Delsemme and Miller (1971). For these two cases the expected value is $R_H \simeq 2\,10^3$ km for 1 mm grains and correspondingly less for smaller grains. Indeed, Hobbs et al. (1975) interpreted their microwave observations of comet Kohoutek at $r = 0.515$ AU as thermal emission of an icy-grain halo with

$$R_H < 0.5\,10^3 \text{ km}.$$

Hence, we conclude that our data represent instead the behaviour of molecular emission, as shown by the excellent fit of the curves labeled *b* in Figures 2 and 3.

The scale lengths obtained by fitting model *b* to our data are listed in Table 1. Assuming that $s_0 \propto r^2$, where r is the heliocentric distance, the scale length reduced to 1 AU is $10^{4.8 \pm 0.1}$ km for comet Bradfield and $10^{5.0 \pm 0.1}$ km for comet Kohoutek. The first figure agrees with $s_0 = 10^{4.80 \pm 0.03}$ km found by Delsemme and Moreau (1973) for the C_2 radical in comet Bennet, while the second is intermediate between that and

$$s_0 = 10^{5.15 \pm 0.03} \text{ km}$$

they found for CN in this comet, both at $r = 1$ AU. Our wideband observations were sensitive both to continuous and band emission; however, in general the visual brightness of the coma is almost entirely due to C_2 emission (Bobrovnikoff, 1951, p. 347). In comet Kohoutek the

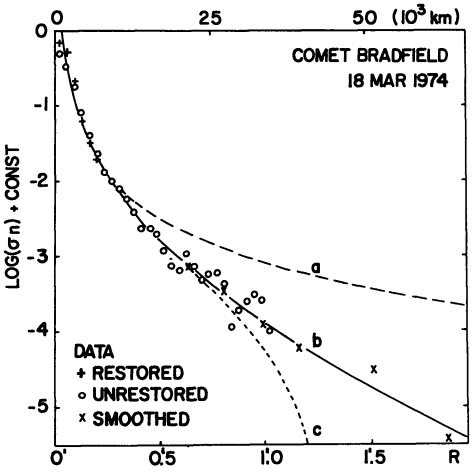

Fig. 2. Run of $\log(\sigma n)$ as a function of distance R to the nucleus for the sunward hemisphere of the coma, when comet Bradfield was at perihelion ($r = 0.50$ AU). Here σ is the cross-section and n is the number density of the particles responsible for the observed light intensity. Data at the fainter light levels have been averaged as described in the text. Theoretical curves are for: *a)* dust model, *b)* molecular emission, and *c)* icy-grain model

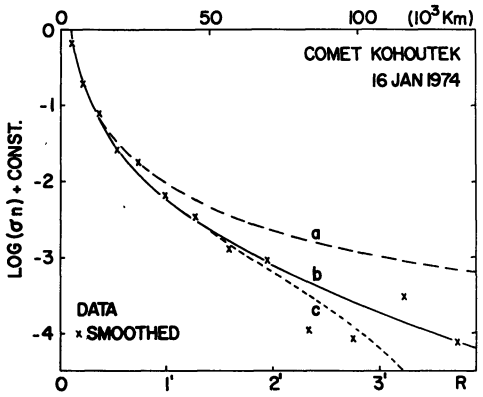

Fig. 3. Same as Figure 2, for comet Kohoutek (1973 XII) at the heliocentric distance $r = 0.68$ AU

C_2 λ5165 band, which was near the effective wavelength of our observations, was quite prominent (A'Hearn, 1975). The radiation of the CN bands in the near UV was strongly absorbed by the large air mass, but it is still possible that their contribution as well as that of the continuum might have been significant, and therefore the agreement with the C_2 scale length of comet Bennet must be treated with caution.

The data confirm the assumption that the effective length of the slit (8') exceeded always (to the sensitivity of our instruments) twice the radius of the coma. On the other hand, the width of the tail was probably greater. Further, the position angle (PA) of the scan was always 90°, with the slit oriented at 0°–180°, while the radius vector of comet Kohoutek was in this period near PA 64° and that of comet Bradfield varied between

PA 84° and 110°. Since a long scan may eventually drift away from the tail, we are not analysing any of our tail data.

In conclusion, we have shown that it is possible to obtain both integrated properties and some idea of cometary structure by using the method of strip photometry.

Acknowledgements. This work was supported in part by the Brazilian Institutions CNPq and BNDE. Computations were performed at the Centro de Processamento de Dados da Universidade Federal do Rio Grande do Sul.

References

A'Hearn, M. F.: 1975, *Astron. J.* **80**, 861
Angione, R. J., Gates, B., Henize, K. G., Roosen, R. G.: 1975, *Icarus* **24**, 111
Baum, W. A.: 1962, *Stars and Stellar Systems* **2**, 1
Bobrovnikoff, N. T.: 1951, *Astrophysics*, Ed. J. A. Hynek McGraw-Hill New York, p. 302
Bracewell, R. N.: 1955, *Australian J. Phys.* **8**, 200
Delsemme, A. H., Miller, D. C.: 1971, *Planetary Space Sci.* **19**, 1229
Delsemme, A. H., Moreau, J. L.: 1973, *Astrophys. Letters* **14**, 181
Hobbs, R. W., Maran, S. P., Brandt, J. C., Webster, W. J. Jr., Swamy, K. S. K.: 1975, *Astrophys. J.* **201**, 749
Houten, C. J. van, Oort, J. H., Hiltner, W. A.: 1954, *Astrophys. J.* **120**, 439
Jacchia, L. G.: 1974, *Sky and Tel.* **47**, 216
Rakos, K. D.: 1965, *Appl. Optics* **4**, 1453
Sawyer-Hogg, H.: 1959, *Hdb. d. Phys.* **53**, 129